III. Theoretical Models

PROTOSTELLAR X-RAYS, JETS, AND BIPOLAR OUTFLOWS

FRANK H. SHU AND HSIEN SHANG
Astronomy Department, University of California
Berkeley, CA 94720-3411, USA

Abstract. We review the theory of x-winds in young stellar objects (YSOs). In particular, we consider how a model where the central star does not corotate with the inner edge of the accretion disk may help to explain the enhanced emission of X-rays from embedded protostars. We argue, however, that the departure from corotation is not large, so a mathematical formulation that treats the long-term average state as steady and axisymmetric represents a useful approximation. Magnetocentrifugally driven x-winds of this description collimate into jets, and their interactions with the surrounding molecular cloud cores of YSOs yield bipolar molecular outflows.

1. Introduction

Beginning with the notion that rapid rotation coupled with strong magnetic fields can considerably enhance the mass loss $\dot{M}_w$ of thermally driven stellar winds (Mestel, 1968), a community effort has gone into the development of the set of ideas comprising the theory of x-winds in YSOs. Even if the resultant flow is quite cold, Hartmann and MacGregor (1982) demonstrated that $\dot{M}_w$ could have almost arbitrarily large values, with the flow velocity at infinity dependent only on the ratio of the azimuthal and radial field strengths at the position where the gas is injected onto open field lines near the equator of a protostar that rotates near breakup. Shu *et al.* (1988) assigned the cause for the protostar to spin at breakup to a circumstellar disk that abuts against the surface of the central object and accretes onto it at a high rate $\dot{M}_D$. They also replaced Hartmann and MacGregor's arbitrary choices for the injection density and angle of magnetic field direction with the requirement that in steady state, the wind mass-loss rate $\dot{M}_w$ and average terminal velcocity $\bar{v}_w$ must be a definite fraction f and multiple

$(2\bar{J}_{\rm w} - 3)^{1/2}$, respectively, of the adjoining disk's accretion rate $\dot{M}_D$ and rotation velocity $\Omega_{\rm x} R_{\rm x}$ (see below).

In the interim, Blandford and Payne (1982) advanced their influential self-similar model of centrifugally driven winds from the surfaces of magnetized accretion disks. Pudritz and Norman (1983) applied these pure disk-wind models to bipolar outflows, and Königl (1989) investigated how the wind might smoothly join a pattern of accretion flow inside the disk. Heyvaerts and Norman (1989) studied how the winds might collimate asymptotically into jets, while Uchida and Shibata (1985) and Lovelace *et al.* (1991) advocated alternative driving mechanisms where magnetic pressure gradients play a bigger role in the acceleration of a disk-blown wind.

Motivated by the problem of binary X-ray sources, a parallel line of research developed concerning how magnetized stars accrete from surrounding disks. Ghosh and Lamb (1978) used order-of-magnitude arguments to show that a strongly magnetized star would truncate the surrounding accretion disk at a larger radius than the stellar radius R_* and divert the equatorial flow along closed field-line funnels toward the polar caps. Although Ghosh and Lamb thought that this inflow would spin up the central object faster than if the accretion disk had extended right up to the stellar surface, Königl (1991) made the surprising and insightful suggestion that the process might torque down the star and account for the relatively slow rate of spin of observed T Tauri stars. Observational support for magnetospheric accretion was subsequently marshalled by Edwards *et al.* (1993) and Hartmann *et al.* (1994).

In a modification of Ghosh and Lamb's ideas based on unpublished work by Arons, McKee, and Pudritz, Arons (1986) proposed that a centrifugally-driven outflow accompanies the funnel inflow [see also Camenzind (1990)]. Independently, Basri (1989, unpublished) had arrived observationally at the same suggestion by extending the synthesis work by Bertout *et al.* (1988) on ultraviolet excesses in T Tauri stars. Shu *et al.* (1994a) put these ideas together into a concrete proposal that generalized the earlier x-wind model of Shu *et al.* (1988).

2. Generalized X-wind Model

In the generalized x-wind model, if the star has mass M_* and magnetic dipole moment μ_*, the gas disk is truncated at an inner radius,

$$R_{\rm x} = \Phi_{\rm dx}^{-4/7} \left(\frac{\mu_*^4}{GM_* \dot{M}_D^2} \right)^{1/7}. \tag{1}$$

A disk of solids may extend inward of $R_{\rm x}$ to the evaporation radius of calcium-aluminum silicates and oxides [see Shang *et al.* (1997) and Meyer

et al. (1997)]. In equation (1), Φ_{dx} is a dimensionless number of order unity that measures the amount of magnetic dipole flux that has been pushed by the disk accretion flow to the inner edge of the disk. In the preferred model of Najita and Shu (1994) and Ostriker and Shu (1995), $\Phi_{dx} = 1.15$, and the actual magnetic flux trapped in a small neighborhood of R_x is 1.5 times larger than the pure dipole value. In other words, magnetic flux is swept toward R_x from both larger and smaller radii (see below).

For a Keplerian disk, the inner edge of the disk rotates at angular speed

$$\Omega_x = \left(\frac{GM_*}{R_x^3}\right)^{1/2}. \qquad (2)$$

To satisfy mass and angular momentum balance, the disk accretion divides at R_x into a wind fraction, $\dot{M}_w = f\dot{M}_D$, and a funnel-flow fraction, $\dot{M}_* = (1 - f)\dot{M}_D$, where

$$f = \frac{1 - \bar{J}_* - \tau}{\bar{J}_w - \bar{J}_*}. \qquad (3)$$

In equation (3) $\bar{J}_*$ and $\bar{J}_w$ are, respectively, specific angular momenta nondimensionalized in units of $R_x^2\Omega_x$ and averaged over funnel and wind streamlines, and τ is the negative of the viscous torque of the disk, $-\mathcal{T}$, acting on its inner edge and measured in units of $\dot{M}_D R_x^2\Omega_x$. For typical application (see below), $\bar{J}_* \approx 0 \approx \tau$ and $\bar{J}_w \approx 3$ or 4; thus, $f \approx 1/3$ or $1/4$. For every gram of material that comes through the disk, the x-wind model requires that a significant fraction gets thrown back out, carrying away the excess angular momentum that the star finds difficult to accept directly.

In steady state, the star is regulated to corotate with the inner disk edge,

$$\Omega_* = \Omega_x. \qquad (4)$$

If corotation did not hold, the system would react to reduce the discrepancy between Ω_* and Ω_x. For example, suppose the star turns faster than the inner edge of the disk, $\Omega_* > \Omega_x$. The field lines attached to both would then continuously wrap into ever tighter trailing spirals, with the field lines adjacent to the star tugging it backward in the sense of rotation. This tug decreases the star's angular rate of rotation Ω_* to more nearly equal the rate Ω_x. Conversely, imagine that $\Omega_* < \Omega_x$. With the star turning slower than the inner edge of the disk, the field lines attached to both would continuously wrap into ever tighter leading spirals, with the field lines adjacent to the star tugging it forward in the sense of rotation. This tug increases the star's angular rate of rotation Ω_*, again to more nearly equal the rate Ω_x. In true steady state, $\Omega_* = \Omega_x$, and the funnel-flow field lines acquire just enough of a trailing spiral pattern (but without continuously wrapping up) so that the excess of material angular momentum brought
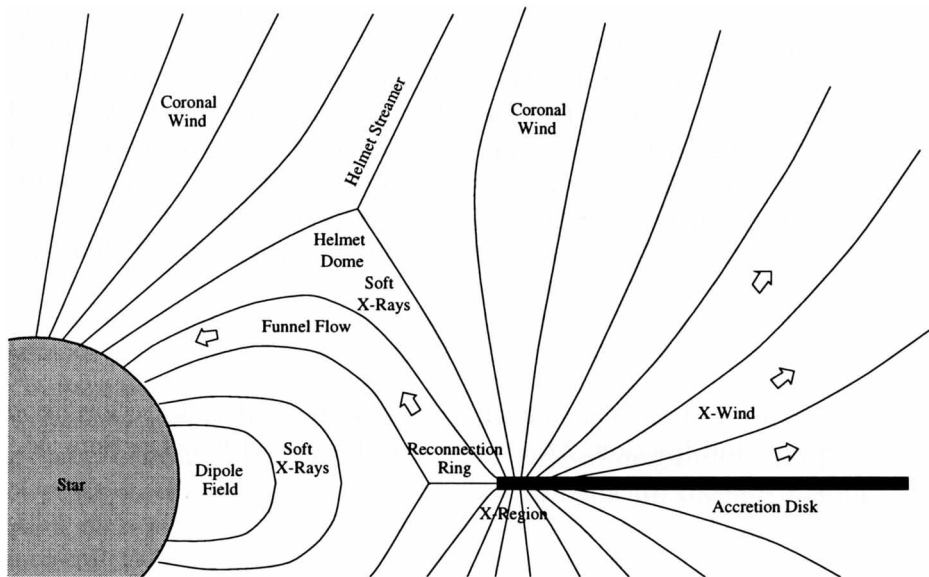
Figure 1. Schematic drawing of the x-wind model. Coronal winds from the star and the disk may help the x-wind to open field lines surrounding the helmet streamer, but this aspect of the configuration is not central to the model.

toward the star by the inflowing gas is transferred outward by magnetic torques to the footpoints of the magnetic field in the disk (Shu *et al.*, 1994a).

The x-wind gas gains angular momentum and the funnel gas loses angular momentum at the expense of the matter at the footpoint of the field in, respectively, the outer and inner parts of the X-region. As a consequence, this matter and the field lines across which it is diffusing pinch toward the middle of the X-region. In reality, Shu *et al.* (1997) point out that the idealized steady state of exact corotation probably cannot be maintained because of dissipative effects. Two surfaces of null poloidal field lines – labeled as "helmet streamer" and "reconnection ring" in Figure 1 – mediate the topological behavior of dipole-like field lines of the star, opened field lines of the x-wind, and trapped field lines of the funnel inflow emanating from the x-region. Across each null surface, which begin or end on "Y-points" [called "kink points" by Ostriker and Shu (1995)], the poloidal magnetic field suffers a sharp reversal of direction. By Ampére's law, large electric currents must flow out of the plane of the Figure along the null surfaces. Nonzero electrical resistivity would lead to the dissipation of these currents and to the reconnection of the oppositely directed field lines [see,

e.g., Biskamp (1993)]. The resultant reduction of the trapped magnetic flux in the x-region as the fan of field lines presses into the evacuated region of the annihilated fields would change the numerical value of the coefficient Φ_{dx} in equation (1).

When R_x changes, the angular speed Ω_x of the footpoint of magnetic field lines in the x-region will vary according to equation (2). However, the considerable inertia of the star prevents its angular velocity Ω_* from changing on the time scale of magnetic reconnection at the null surfaces of the magnetosphere. The resultant shear when $\Omega_* \neq \Omega_x$ will stretch and amplify field lines attached to both the star and the disk. The poloidal field will bulge outward from the increased magnetic pressure, inserting more magnetic flux into the fan of field lines emanating from the x-region [see the simulations of Linker and Mikić (1994) and Hayashi *et al.* (1996)]. Dynamo action inside the star would presumably replace the upward rising dipole-like poloidal fields. This dynamo action would be enhanced by the wrapping of field lines between the star and disk. Averaged over long times, we envisage a secular balance, with enough dynamo-generated poloidal field being inserted into the x-region to balance the rate of field dissipation at the null surfaces.

Johns and Basri (1995) and Johns-Krull and Hatzes (1997) have found two sources in which the hydrogen lines that diagnose for inflow and outflow exhibit a periodicity equal to the rotation period of the central T Tauri star. If the funnel flow and wind emanate in these objects from the surrounding accretion disks, then the source regions for the flowing gas corotate with the central stars – in agreement with the prediction that $\Omega_* = \Omega_x$. However, the majority of objects studied by Johns-Krull and Basri (1997) do not show such periodicity, indicating that even if Ω_* does equal Ω_x as a long-term average, Ω_* may not generally equal Ω_x instantaneously.

3. Evidence from Protostellar X-rays

Recent X-ray observations of YSOs may yield important constraints on the degree by which Ω_* does not equal Ω_x. Comparing data from *ROSAT* and *ASCA*, Carkner *et al.* (1996) find that the X-ray spectra of classical T Tauri stars (CTTSs) are harder than weak-lined T Tauri stars (WTTSs) (Feigelson *et al.*, 1987), but not as hard as embedded protostars (Koyama *et al.*, 1996). The luminosity of low-mass protostars at all X-ray energies is typically [see Grosso *et al.* (1997) and the discussion in note 11 of Shu *et al.* (1997)]:

$$L_x^{tot} \sim 1 \times 10^{32} \text{ erg s}^{-1}, \tag{5}$$

which is about 2 orders of magnitude larger than the corresponding values for WTTSs and CTTSs. Since a main difference among these objects is

the rate of disk accretion, it is tempting to attribute the enhanced X-ray emission in protostars to the strong interaction between the stellar magnetosphere and the surrounding accretion disk [see also Hayashi *et al.* (1996) and Goodson *et al.* (1997)].

When $\Omega_* \neq \Omega_x$, Shu *et al.* (1997) use dimensional analysis to estimate the rate of increase of magnetic energy in field lines attached to both the star and the x-region:

$$\frac{dE_{\text{mag}}}{dt} = \alpha|\Omega_* - \Omega_x|\frac{\mu_*^2}{R_x^3}, \tag{6}$$

where α is a numerical coefficient of order unity. Numerical calculations suggest that coronal mass ejections occur when the field energy increases to a point where erupting magnetized plasmoids can open the field lines under the helmet dome [see the simulation of solar flares in Figures 1 and 2 of Linker and Mikić (1994)]. As previewed in the previous section, the analogous process in the reconnection ring will sporadically inject fresh poloidal fields to offset the reconnection loss of trapped magnetic flux in the x-region.

We write $|\Omega_* - \Omega_x|$ as a fraction S of Ω_x. Using equations (1) and (2) to eliminate μ_* and Ω_x, we then get

$$\frac{dE_{\text{mag}}}{dt} = (\alpha S \Phi_{\text{dx}}^2)\frac{GM_*\dot{M}_D}{R_x}. \tag{7}$$

For low-mass protostars, the quantity $GM_*\dot{M}_D/R_x$ has a typical order of magnitude of 3×10^{33} erg s^{-1}. Thus, if the time-averaged X-ray luminosity L_x^{tot} in equation (5) is ultimately supplied by the time-averaged release of magnetic energy dE_{mag}/dt, and if α and $\Phi_{\text{dx}} \sim 1$, then equation (7) allows us to estimate that $S \sim 0.03$. This represents a small average departure from corotation. While such instantaneous departures may be important in understanding the short-term variability and eruptive magnetic activity, we henceforth ignore them for the long-term behavior of YSOs.

4. Outline of Mathematical Formulation

A mathematical formulation of the steady-state problem when $\Omega_* = \Omega_x$ was given in outline by Shu *et al.* (1988) and in detail by Shu *et al.* (1994b), who nondimensionalized the governing equations by introducing R_x, Ω_x^{-1}, and $\dot{M}_w/4\pi R_x^3\Omega_x$, respectively, as the units of length, time, and density. Assuming axial symmetry and time-independence in a frame that corotates with Ω_x, we may then introduce cylindrical coordinates (ϖ, φ, z) and a stream-function $\psi(\varpi, z)$ that allows the satisfaction of the equation of continuity,

$\nabla \cdot (\rho \mathbf{u}) = 0$, in the meridional plane:

$$\rho u_\varpi = \frac{1}{\varpi} \frac{\partial \psi}{\partial z}, \qquad \rho u_z = -\frac{1}{\varpi} \frac{\partial \psi}{\partial \varpi}. \tag{8}$$

Field freezing in the corotating frame, $\mathbf{B} \times \mathbf{u} = 0$, implies that the magnetic field is proportional to the mass flux, $\mathbf{B} = \beta \rho \mathbf{u}$, where β is a scalar. The condition of no magnetic monopoles, $\nabla \cdot \mathbf{B} = 0$, now requires that β be conserved on streamlines, *i.e.*,

$$\beta = \beta(\psi). \tag{9}$$

Similarly, the conservation of total specific angular momentum requires that the amount carried by matter in the laboratory frame, $\varpi(\varpi \Omega_x + u_\varphi)$ where Ω_x is replaced by 1 in dimensionless equations, plus the amount carried by Maxwell torques, $-\varpi B_\varphi \mathbf{B}$, per unit mass flux, $\rho \mathbf{u}$, equals a function of ψ alone:

$$\varpi[(\varpi + u_\varphi) - \beta^2 \rho u_\varphi] = J(\psi). \tag{10}$$

Finally, conservation of specific "energy" in the corotating frame for a gas with dimensionless isothermal sound speed ϵ results in Bernoulli's theorem:

$$\frac{1}{2}|\mathbf{u}|^2 + \mathcal{V}_{\text{eff}} + \epsilon^2 \ln \rho = H(\psi). \tag{11}$$

Up to an arbitrary constant, defined so that $\mathcal{V}_{\text{eff}} = 0$ at the x-point $\varpi = 1$ and $z = 0$, $\mathcal{V}_{\text{eff}}$ is the dimensionless gravitational potential plus centrifugal potential (measured in units of $GM_*/R_x = \Omega_x^2 R_x^2$):

$$\mathcal{V}_{\text{eff}} = \frac{3}{2} - \frac{1}{(\varpi^2 + z^2)^{1/2}} - \frac{\varpi^2}{2}. \tag{12}$$

Equations (9) - (11), with β, J, and H arbitrary functions of ψ, represent formal integrations of the governing set of equations. The remaining equation for the transfield momentum balance – the so-called Grad-Shafranov equation – cannot be integrated analytically and reads

$$\nabla \cdot (\mathcal{A} \nabla \psi) = \mathcal{Q}, \tag{13}$$

where $\mathcal{A}$ is the Alfvén discriminant,

$$\mathcal{A} \equiv \frac{\beta^2 \rho - 1}{\varpi^2 \rho}, \tag{14}$$

and $\mathcal{Q}$ is a source function for the internal collimation (or decollimation) of the flow:

$$\mathcal{Q} = \rho \left[\frac{u_\varphi}{\varpi} J'(\psi) + \rho |\mathbf{u}|^2 \beta \beta'(\psi) - H'(\psi) \right], \tag{15}$$

with primes denoting differentiation with respect to the argument ψ.

The quantity $\mathcal{A} = 0$, $i.e.$, $\beta^2 \rho = 1$, when the square of the flow speed $|\mathbf{u}|^2$ equals the square of the Alfvén speed, $|\mathbf{B}|^2/\rho$. For sub-Alfvénic flow, $\mathcal{A} > 0$; for super-Alfvénic flow, $\mathcal{A} < 0$. If $\mathcal{A}$ were freely specifiable (which it is not), equation (13) would resemble the time-independent heat-conduction equation. What is spreading in the meridional plane of our problem, however, is not heat, but streamlines.

5. Fixing the Free Functions

When combined with Bernoulli's equation (11), the Grad-Shafranov equation (13) has three possible critical surfaces associated with it, corresponding to slow MHD, Alfvén, and fast MHD crossings (Weber and Davis, 1967). Thus, when applied to the problem of the x-wind, equation (13) is a second-order partial differential equation of elliptic type interior to the fast surface and hyperbolic type exterior to this surface [see Heinemann and Olbert (1978) and Sakurai (1985)]. The unknown functions $\beta(\psi)$, $J(\psi)$, and $H(\psi)$ are to be determined self-consistently so that the three crossings of the critical surfaces are made smoothly. This does not fix all three functions uniquely since the loci of the critical surfaces in (ϖ, z)-space are not known in advance. It turns out that we can choose one of the loci freely. Alternatively, we can freely specify one of the functions β, J, or H. The method of Najita and Shu (1994) fixes in advance the locus of the Alfvén surface and determines all other quantities self-consistently from this parameterization. Shang and Shu (1997) have invented a simplified procedure in which the function $\beta(\psi)$ is specified in advance; then $J(\psi)$, $H(\psi)$, and the loci of the slow, Alfvén, and fast surfaces are found as part of the overall solution (including force balance with the opened field lines of the star and dead zone). We may regard the procedure of choosing $\beta(\psi)$ arbitrarily as a mathematical substitute for the physical problem, where loading of matter onto field lines occurs in the x-region with the breakdown of the ideal MHD approximation of field freezing (Shu et $al.$, 1994a).

Apart for a trivial replacement of $\dot{M}_*$ for $\dot{M}_{\mathrm{w}}$, the funnel flow behaves somewhat differently from the x-wind. The funnel flow has a slow MHD crossing but probably no Alfvén or fast MHD crossings. (In steady state the star and disk can communicate with each other along closed field lines by means of the latter two signals.) As a consequence, both $\beta(\psi)$ and $J(\psi)$ can be freely specified for the funnel flow, although $J(\psi)$ must ultimately be made self-consistent with the physical assumption that no spinup or spindown of the star occurs in steady state, $i.e.$, that Ω_* remains equal to Ω_{x} as a long-term average. In these circumstances, when one has a small star, Ostriker and Shu (1995) show that $J(\psi)$ is likely to be nearly zero

on every funnel-flow streamline $\psi = $ constant. In other words, $\bar{J}_* \approx 0$ and any excess angular momentum brought to the star by the matter inflow is transferred back to the disk by the magnetic torques of a trailing spiral pattern of funnel field lines.

6. The Cold Limit

The overall problem is mathematically tractable because the parameter ϵ is much smaller than unity (typically, $\epsilon \approx 0.03$). This leads to many simplifications, in particular, to the use of matched asymptotic expansions for solving and connecting different parts of the flow. For example, we may show that the slow MHD crossing must be made by matter-carrying streamlines within a fractional distance ϵ of R_x (unity in our nondimensionalization), and that to order ϵ^2, $H(\psi)$ may be approximated as zero. In the limit $\epsilon \to 0$, the gas that becomes the x-wind (or the funnel flow) emerges with linearly increasing velocities in a fan of streamlines from the X-region as if it were a single point.

In this approximation, the function $\beta(\psi)$ cannot be chosen completely arbitrarily if the magnetic field, mass flux, and mass density do not to diverge on the uppermost streamline $\psi \to 1$ as the x-wind leaves the x-region. For modeling purposes, Shang and Shu (1997) adopt the following distribution of magnetic field to mass flux:

$$\beta(\psi) = \beta_0 (1 - \psi)^{-1/3}, \tag{16}$$

where β_0 is a numerical constant related to the mean value of β averaged over streamlines:

$$\bar{\beta} \equiv \int_0^1 \beta(\psi)\, d\psi = \frac{3}{2}\beta_0. \tag{17}$$

The reader should not worry that equation (16) implies $\beta \to \infty$ as $\psi \to 1$. This singular behavior merely reflects the fact that the magnetic field $\mathbf{B} = \beta\rho\mathbf{u}$ is nonzero on the last x-wind streamline where by definition ρ must become vanishingly small while $\mathbf{u}$ remains finite.

7. Asymptotic Collimation into Jets

Given the form $\beta(\psi)$ from equation (16), the loci of streamlines at large distances from the origin may be recovered in spherical polar coordinates $[r = (\varpi^2 + z^2)^{1/2}, \theta = \arctan(\varpi/z)]$ from the asymptotic analysis of Shu *et al.* (1995):

$$r = \frac{2\bar{\beta}}{C}\cosh[F(C,1)], \qquad \sin\theta = \mathrm{sech}[F(C,\psi)], \tag{18}$$

where different values of the dimensionless current C correspond to different locations on any streamline $\psi = \text{constant}$, and where $F(C, \psi)$ is the integral function,

$$F(C, \psi) \equiv \frac{1}{C} \int_0^\psi \frac{\beta(\psi)\, d\psi}{[2J(\psi) - 3 - 2C\beta(\psi)]^{1/2}}. \qquad (19)$$

Notice that $r \to \infty$ when $C \to 0$ and *vice-versa*.

The factor $2\bar{\beta}$ in equation (18) applies if the field lines in the dead zone are completely closed as assumed in the calculations of Ostriker and Shu (1995) and Shu *et al.* (1995), but it becomes $6\bar{\beta}$ if they are completely opened as in Figure 1 [see the discussion of Shang and Shu (1997)]. In the former case, the hoop stresses of the toroidally wrapped fields on the uppermost streamlines of the x-wind are asymptotically balanced by the magnetic pressure of a bundle of longitudinal field lines coming from the star that carries the same dimensionless magnetic flux, $2\pi\bar{\beta}$, as their opened counterparts in the x-wind. In the latter case, there are additional longitudinal field lines roughly parallel and antiparallel to the polar axis carrying oppositely directed flux $\pm 2\pi\bar{\beta}$ from the opened field lines of the dead zone. The general case would have a coefficient in equation (18) between $2\bar{\beta}$ and $6\bar{\beta}$.

The density and velocity fields associated with equation (18) are obtained from

$$\rho = \frac{C}{\beta\varpi^2}, \qquad v_{\text{w}} = (2J - 3 - 2C\beta)^{1/2}, \qquad (20)$$

where $\varpi \equiv r\sin\theta$ and v_{w} is the wind speed in an inertial frame. The solid and short dashed lines in Figure 2 show, respectively, isodensity contours and flow streamlines for a case $\beta_0 = 1$ computed on four different scales by the simplified approximate procedure discussed by Shang and Shu (1997). The dimensional units of length and velocity, R_{x} and $\Omega_{\text{x}} R_{\text{x}}$, are ~ 0.06 AU and ~ 100 km s^{-1} in typical application. The outermost density contour in the fourth panel is $\rho = 10^{-8}$ in units of $\dot{M}_{\text{w}}/4\pi\Omega_{\text{x}} R_{\text{x}}^3$. For the model $\bar{J}_{\text{w}} = 3.73$, as can be obtained from the square of the average ϖ position of the inner set of long dashes marking the location of the Alfven surface. The Alfvén and fast surfaces formally asymptote to infinity as the upper streamline $\psi = 1$ is approached, where the density becomes vanishingly small. Because numerical computations are difficult in this limit, the actual uppermost streamline displayed is $\psi = 0.98$ rather than $\psi = 1$. Although streamlines collimate logarithmically slowly, isodensity contours become cylindrically stratified fairly quickly, roughly as $\rho \propto \varpi^{-2}$ [*cf.* equation (20)]. Since the radiative emission of forbidden lines is highly biased toward regions of moderately high density, the flow will appear more collimated than it actually is. There is a greater wide-angle component to YSO
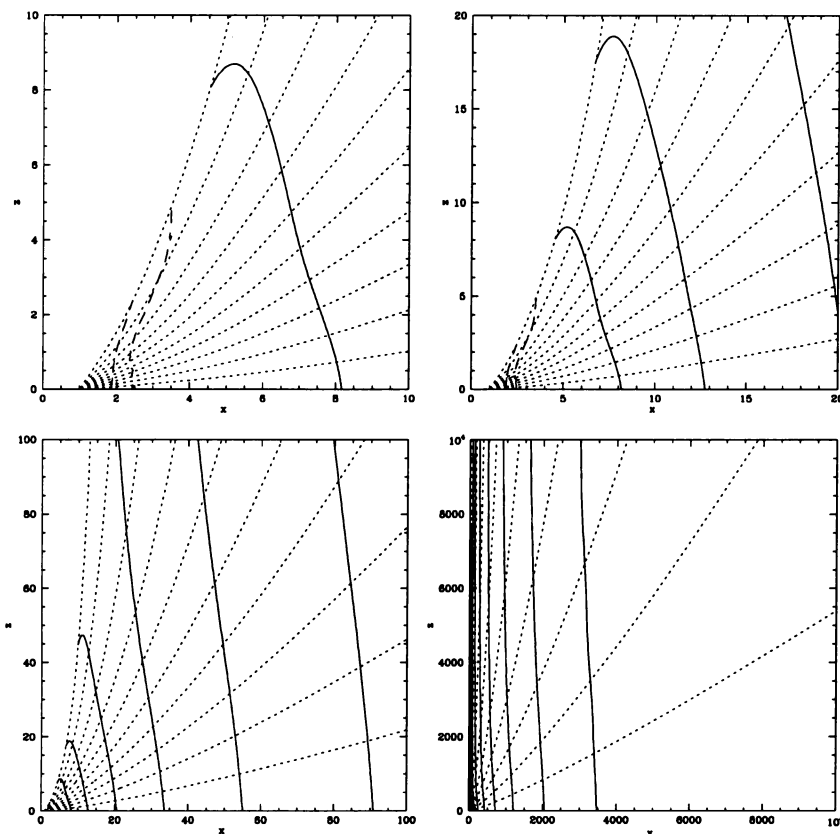
Figure 2. Isodensity contours (solid curves) and streamlines (dotted curves) for a cold x-wind with $\beta(\psi) = \beta_0(1 - \psi)^{-1/3}$, where $\beta_0 = 1$. Isodensity contours are spaced logarithmically in intervals of $\Delta \log_{10} \rho = 0.5$, and streamlines are spaced so that successive dotted lines contain an additional 10% of the total mass loss in the upper hemisphere of the flow. The loci of the Alfvén and fast surfaces are marked by dashed lines. The empty space inside the uppermost streamline, $\varpi \leq \varpi_1$, is filled with open field lines from the central star that asymptotically have the field strength, $B_z = 2\bar{\beta}/\varpi_1^2$.

winds than generally appreciated. In other words, the jetlike appearance of YSO outflows is somewhat of an optical illusion.

The relative lack of streamline collimation, as opposed to density collimation, is a salient feature of the x-wind model and provides a key discriminating test via spectroscopy of forbidden line emission at high spatial and spectral resolution. The x-wind model predicts that such lines should have

larger velocity widths at the base of the flow, where a typical line of sight encounters flow velocities at a variety of angles, than farther up the length of the jet, where the flow vectors are better oriented along a single direction. A hint of this behavior may already be present in the data presented by Solf at this conference.

8. Bipolar Molecular Outflows

Shu *et al.* (1991) proposed that bipolar molecular outflows are created when a YSO wind with power dependent on polar angle θ as $P(\theta)$ sweeps up static ambient material with a density distribution (generated by ambipolar diffusion) given by

$$\rho_{\mathrm{amb}}(r, \theta) = \frac{a^2 Q(\theta)}{2\pi G r^2}, \tag{21}$$

where a is the effective isothermal sound speed of the surrounding molecular cloud core and $Q(\theta)$ describes the flattening produced by magnetic forces. Li and Shu (1996) have computed the resulting model when $P(\theta) \propto 1/\sin^2 \theta$ as predicted by the asymptotic analysis of the previous section and when $Q(\theta)$ of the theoretical molecular cloud core (a self-gravitating magnetized toroid) is chosen to be consistent with the observational data on core flattening (Myers *et al.*, 1991). They show that the model, which has *no* adjustable parameters in nondimensional form, gives surprisingly good recreations of the observations concerning lobe shapes, line profiles, distributions of mass with line-of-sight velocities, and distributions of momenta with bipolar axial distance (Chernin and Masson, 1995). Given the simplicity of the model, where the real magnetohydrodynamics is collapsed into a single thin-shell treatment, the agreement is quite encouraging, especially in light of the difficulty that more complex (and also more *ad hoc*) jet-driven models have traditionally had in explaining the same data (see the discussions of Cabrit *et al.* and Eislöffel in this volume).

9. Stability of Parsec Long Jets

The small amount of ambient matter swept to high velocities, which solves the original objection of Masson and Chernin (1992) to the bipolar outflow model of Shu *et al.* (1991), arises because the heaviest part of the x-wind encounters only the low-density material of the poles of the molecular toroid [where $Q(\theta)$ ideally becomes vanishingly small]. As a consequence, it is easy for the x-wind to break out of the molecular cloud core in these directions and, thus, to account for the parsec long jets presented by Bally at this conference.

It has often been asked how jets can maintain their integrity for such long paths. The glib answer provided by all proponents of magnetocentrifugal driving is that the flow is self-collimated. Self-collimation occurs by the hoop stresses of the toroidal magnetic fields that grow in relative strength to the poloidal components as the flow distance from the source increases. But such magnetic confinement schemes have long been known to the fusion community to be unstable with respect to kinking and sausaging [see Figure 10.6 in Jackson (1975); see also Eichler (1993)]. A solution to the problem has also long been known and is the principle behind working Tokamaks: the introduction of dynamically important levels of longitudinal magnetic fields along the length of the plasma column to stabilize the kinking and sausaging motions [see Figures 10.7 and 10.8 of Jackson (1975)]. Such dynamically important levels of longitudinal fields along the central flow axis are exactly what fill the hollow core of the jet in the x-wind model of Figure 2.

10.   Crushing the Magnetosphere?

At this conference, Hartmann has questioned the applicability of x-wind models to YSO jets and bipolar outflows on the basis that the mass accretion rate $\dot{M}_D$ in the most active sources should be large enough to crush the magnetosphere to the stellar surface. His argument proceeds by assuming that every quantity in equation (1) is fixed at the same value in different sources except for $\dot{M}_D$. He scales according to CTTSs where $R_x \sim 5R_*$ after he has lowered $\dot{M}_D$ in CTTSs by a factor of 10 from the conventionally estimated values [see Bertout (1989) and Edwards et al. (1993)]. He then finds R_x to be smaller than R_* for sources in which $\dot{M}_D$ is appreciably larger than the value he adopts for CTTSs.

Clearly, more debate and re-evaluation is needed to assess the validity of the lower $\dot{M}_D$ adopted for CTTSs. Even if we accept the proposition, a weak point exists in the supposition that everything else on the right-hand side of equation (1) retains the same value in different sources. Consider the objects most likely to have crushed stellar magnetospheres – sources in FU Orionis outburst. During an FU Orionis outburst, $\dot{M}_D$ may indeed increase from the quiescent state by a few orders of magnitude. The increase in $\dot{M}_D$ should result initially in a decrease in R_x. But, in accordance with equation (6), the resulting mismatch in Ω_x and Ω_* will generate on the shear time scale a substantial increase in the magnetic energy of the configuration. This increase inserts more trapped magnetic flux into the x-region (and thereby increasing the coefficient $\Phi_{dx}^{-4/7}$). Through enhanced dynamo action, it may also increase the stellar magnetic dipole moment μ_* (thus also increasing R_x relative to Hartmann's scaling). Hence, it may not be so easy, even in the

case of FU Orionis outbursts, to completely crush a stellar magnetosphere by disk accretion. A substantial portion of the outer layers of the star (the part that anchors the magnetic field) may have to be spun to breakup (so that Ω_* effectively equals Ω_x, shutting off the enhanced dynamo) before the stellar magnetosphere can be crushed. But such a situation reproduces precisely the assumption underlying the original x-wind model (Shu *et al.*, 1988), so an x-wind can still be launched in this case.

Finally, we note that a departure of Ω_* from Ω_x has no effect on the generalized theory of x-winds reviewed in this paper, since the field lines in the x-wind are disconnected from those of the star (see Figure 1). As long as the base of the x-wind rotates at or close to the Keplerian speed Ω_x given by equation (2), the footpoint of the field will have the necessary centrifugal fling to drive an x-wind. What will be affected by $\Omega_* \neq \Omega_x$ is the time-steady assumption for the funnel flow. As we have argued, the main modification may be a time-unsteady response that results in a transient amplification of the magnetic field.

References

Arons, J. 1986, in Plasma Penetration into Magnetospheres, ed. N. Kylafis, J. Papamas-torakis, and J. Ventura (Iraklion: Crete Univ. Press), 115

Bertout, C. 1989, ARAA 27, 351

Bertout, C., Basri, G., and Bouvier, J. 1988, ApJ 330, 350

Biskamp, D. 1993, Nonlinear Magnetohydrodynamics (Cambridge University Press)

Blandford, R.D., and Payne, D.G. 1982 MNRAS 199, 883

Camenzind, M. 1990, in Reviews in Modern Astronomy 3, ed. G. Klare (Berlin: Springer), 259

Carkner, L. Feigelson, E.D., Koyama, K., Montmerle, T, and Reid, I.N. 1996, ApJ 464, 286

Chernin, L., and Masson, C. 1995, ApJ 455, 182

Edwards, S., Strom, S. E., Herbst, W., Attridge, J., Merrill, K. M., Probst, R., and Gatley, I. 1993, AJ 106, 372.

Eichler, D. 1993, ApJ 419, 111

Feigelson, E.D., Jackson, J.M., Mathieu, R.D., Myers, P.C., and Walter, F.M. 1987, AJ 94, 1251

Ghosh, P., and Lamb, F.K. 1978, ApJ 223, L83

Goodson, A.P., Winglee, R.M., and Böhm, K.-H. 1997, ApJ, submitted

Grosso, N., Montmerle, T., Feigelson, E.D., André. P., Casanova, S., and Gregorio-Hetem, J., Nature, in press

Hartmann, L., Hewitt, R., and Calvet, N. 1994, ApJ 426, 669

Hartmann, L., and MacGregor, K.B. 1982, ApJ 259, 180.

Hayashi, M.R., Shibata, K., and Matsumoto, R. 1996, ApJ 468, L37

Heinemann, M., and Olbert, S. 1978, J. Geophys. Res. 83, 2457

Heyvaerts, J., and Norman, C. 1989, ApJ 347, 1055

Jackson, J.D. 1975, Classical Electrodynamics (New York: Wiley)

Johns, C.M., and Basri, G. 1995, ApJ 449, 341

Johns-Krull, C.M., and Basri, G. 1997, ApJ 474, 443

Johns-Krull, C.M., and Hatzes, A.P. 1997, ApJ, in press

Königl, A. 1989, ApJ 342, 208

Königl, A. 1991, ApJ 370, L39

Koyama, K., Ueno, S., Kobayashi, N., and Feigelson, E.D. 1996, PASJ 48, L87

Li, Z.Y., and Shu, F.H. 1996, ApJ 472, 211

Linker, J. A., and Mikić, Z. 1994, ApJ 430, 898

Lovelace, R.V.E, Berk, H.L., and Contopoulos, J. 1991, ApJ 379, 696

Masson, C., and Chernin, L. 1992, ApJ 387, L47

Mestel, L. 1968, MNRAS 138, 359

Meyer, M.R., Calvet, N., and Hillenbrand, L.A. 1997, AJ, in press.

Myers, P.C., Fuller, G.A., Goodman, A.A., and Benson, P.J. 1991, ApJ 376, 561

Najita, J.R., and Shu, F.H. 1994, ApJ 429, 808

Ostriker, E.C., and Shu, F.H. 1995, ApJ 447, 813

Pudritz, R.E., and Norman, C.A. 1983, ApJ 274, 677

Sakurai, T. 1985, A&A 152, 121

Shang, H., Shu, F., Lee, T., and Glassgold, A.E. 1997, in Low Mass Star Formation from Infall to Outflow, Poster Proc. IAU Symp. No. 182, ed. F. Malbet and A. Castets (Grenoble: Laboratorie d'Astrophysique), 312

Shang, H., and Shu, F.H. 1997, in preparation

Shu, F.H., Lizano, S., Ruden, S., and Najita, J. 1988, ApJ 328, L19

Shu, F.H., Ruden, S.P., Lada, C.J., and Lizano, S. 1991, ApJ 370, L31

Shu, F., Najita, J., Ostriker, E., Wilkin, F., Ruden, S., and Lizano, S. 1994a, ApJ 429, 781

Shu, F.H., Najita, J., Ruden, S.P., and Lizano, S. 1994b, ApJ 429, 797

Shu, F.H., Najita, J., Ostriker, E. C., and Shang, H. 1995, ApJ 455, L155

Shu, F.H., Shang, H., Glassgold, A.E., and Lee, T. 1997, Science, submitted.

Uchida, Y., and Shibata, K. 1985, PASJ 37, 515

Weber, E.J., and Davis, L. 1967, ApJ 148, 217